DOI: 10.1002/ejoc.200500725

Alkoxyamine C–ON Bond Homolysis: Stereoelectronic Effects

Emmanuel Beaudoin,[a] Denis Bertin,[a] Didier Gigmes,[a] Sylvain R. A. Marque,*[a] Didier Siri,[a] and Paul Tordo[a]

In memory of Professor Hanns Fischer[‡]

Keywords: Alkoxyamines / Density functional calculations / Linear free energy relationships / Through-space interactions / Structure elucidation

Alkoxyamines and persistent nitroxides are important regulators of nitroxide-mediated radical polymerization (NMP) reactions. Because polymerization times decrease with an increase in the rate constant for the homolysis of the C–ON bond between the polymer chain and the nitroxyl moiety, the factors influencing the cleavage rate constant are of considerable interest. Therefore, it was interesting to check whether the methyl effect (+17 kJ/mol for each methyl added onto the carbon atom of the C–ON bond) observed in the TEMPO-based alkoxyamine series was also observed in the SG1 [*N*-*tert*-butyl-*N*-(1-diethoxyphosphoryl-2,2-dimethylpropyl)aminoxyl] series. Moreover, we extended the incremental substituent scale proposed earlier and confirmed the versatility of the multiparameter analysis developed in previous work. X-ray and natural bond orbital (NBO) analyses of several SG1-CHMeCOOR alkoxyamines showed that the difference in reactivity between the (*RR*/*SS*) and (*RS*/*SR*) diastereoisomers is caused by a $n_\sigma \rightarrow \sigma^*$ interaction between the n_σ lone pair of the oxygen atom of the ester bond and the σ^* orbital of the cleaved O–C bond. Furthermore, a compilation of the effects – steric, polar, stabilizing, long-distance polar and long-distance reverse steric – of the leaving alkyl radical on the value of k_d for C–ON bond homolysis led us to question the one-step mechanism.

Introduction

A decade ago, Rizzardo[1] and Georges[2] and their coworkers showed that it was possible to prepare well-defined polymers using nitroxyl radicals or alkoxyamines as controllers. Nitroxide-mediated polymerization (NMP) was born[3,4] and it has inspired numerous studies, carried out to elucidate the mechanism[5] and kinetics of polymerization,[6–11] to prepare new polymers[3,12–14] and to develop more efficient initiators/controllers.[15–22] Scheme 1 depicts a simplified[23] NMP process, with k_d the rate constant for C–ON bond homolysis in the alkoxyamine (the so-called dormant species), k_c the rate constant for the reformation of the alkoxyamine, k_p the propagation rate constant for the polymerization reaction and k_t the self-termination rate constant.

Recent results obtained by our group[20,23] showed that the initiating step, that is, the value of k_d, is of the highest importance for the successful control and quality [low polydispersity index (PDI), high livingness] of the NMP process. For example, the polymerization reaction can be initiated only with alkoxyamines that react at least as fast as the model alkoxyamine and exhibit the right value of the preequilibrium constant *K*. However, this does not ensure successful NMP.[6–11] Indeed, the NMP of the *n*-butyl acrylate monomer initiated with **9** (Figure 1) or similar alkoxyamines requires the addition of free nitroxyl radicals to control the polymerization as a result of the large value of k_p. The same polymerization reactions carried out with the tertiary alkoxyamines presented in this paper were performed without adding free nitroxyl radicals. Furthermore, the control was observed from 10 up to 80% conversion whereas the control is, in general, observed only above 30% conver-

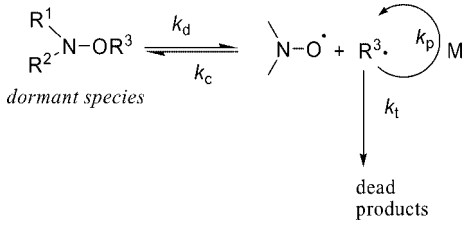

Scheme 1.

[a] UMR 6517 case 542, Université de Provence,
Avenue Escadrille Normandie-Niemen, 13397 Marseille Cedex 20, France
Fax: +33-4-91288758
E-mail: sylvain.marque@up.univ-mrs.fr
[‡] Deceased February 22, 2005.
Supporting information for this article is available on the WWW under http://www.eurjoc.org or from the author.

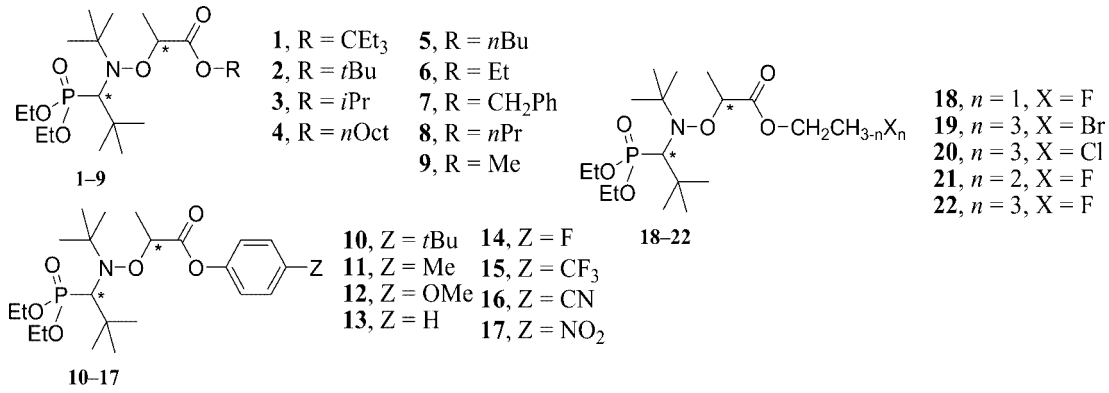

Figure 1. Structures of SG1-based alkoxyamines exhibiting long-range steric and polar effects.

sion.[20,23] Moreover, the amount of added nitroxyl radicals depends a great deal on the experimental conditions which is a major drawback for the scaling-up of this technique to the industrial scale. On the other hand, a monocomponent system based on the fast homolysis of tertiary alkoxyamines helps overcome this problem.

Alkoxyamines ($R^1R^2NOR^3$) are the key intermediates[5] of NMP and the strength of the C–ON bond is a crucial parameter for its control.[5–11] It has been shown that the activation energy (E_a) of the homolysis step is a good estimate of the value of the bond dissociation energy (BDE) of the C–ON bond.[24,25] We and others have shown that the C–ON bond in alkoxyamines is either strengthened by anomeric[26,27] (due to, for example, a heteroatom bound to the carbon) and polar effects[24,27–30] [due to an electron-withdrawing group (EWG) bound to the nitrogen atom] or weakened by the steric strain and polar effects of both alkyl and nitroxyl fragments.[15,17,21,24,26,31–35] Furthermore, stabilization[24,26–28,31,33] of the released alkyl and nitroxyl radicals[27,29] – stabilized by an intramolecular hydrogen bond – also weakens the C–ON bond. A few years ago, studies[24] on TEMPO (2,2,6,6-tetramethylpiperidin-*N*-oxyl)-based alk-

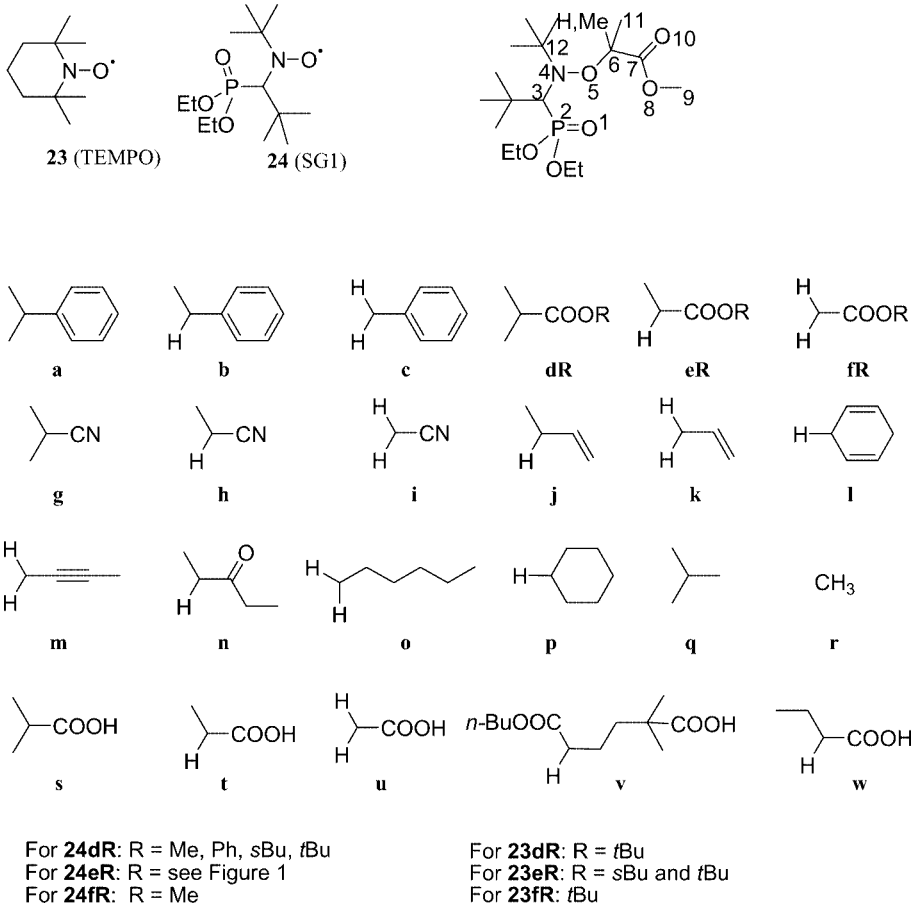

Figure 2. Structures of the alkyl and nitroxyl fragments composing the alkoxyamines of type **23** and **24**.

oxyamines showed that the presence of a methyl group on the carbon atom of the C–ON bond reduces the activation energy of homolysis by roughly 17 kJ/mol. Up to now, this effect has only been clearly observed with TEMPO-based alkoxyamines. Recently, we examined the effect of the ester group on the k_d of SG1 [*N*-*tert*-butyl-*N*-(1-diethoxyphosphoryl-2,2-dimethylpropyl)aminoxyl]-CHMeCOOR alkoxyamines (Figure 1) and observed that both diastereoisomers exhibited sensitivities similar to the long-range reverse steric effect[36,37] − decreasing k_d with increasing size of the ester group − and different to the long-range polar effect.[35] With the new alkoxyamines **24g**, **24dMe**, **24dPh**, **24u** and **24v**, we present herein the first complete series of SG1-based alkoxyamines (primary, secondary and tertiary alkyl groups, Figure 2). We also present a more complete incremental substituent scale and a multiparameter analysis that includes the tertiary alkyl SG1-based alkoxyamines and a few other new ones. These are useful tools for pre-estimating the activation energy of the homolysis step and thus the values of the homolysis rate constant k_d. Based on X-ray structures [**24dPh**, **24s**, (*RR*/*SS*)- and (*RS*/*SR*)-**17**, (*RS*/*SR*)-**24eMe**] and Natural Bond Orbital (NBO) analyses [(*RS*/*SR*)- and (*RR*/*SS*)-**24eMe** and (*RR*/*SS*)- and (*RS*/*SR*)-**2**], we propose a stereoelectronic effect ($n_\sigma \rightarrow \sigma^*$ interaction) to account for the differences in reactivity observed for several diastereoisomers of SG1-based alkoxyamines.

Unfortunately, not all derivatives of the two nitroxyl radicals were available. Alkyl fragments **a**, **b**, **dR**, **eR**, **g**, **h**, **j**, **p**, **q**, **s** and **t** should be reasonable models for the propagating radicals of α-methylstyrene, styrene, methacrylates, acrylates, methacrylonitrile, acrylonitrile, butadiene, ethylene, isoprene, methacrylic and acrylic acid, respectively, provided a weak penultimate effect occurs. For the sake of conciseness, not all the kinetic parameters for all the alkoxyamines are reported in Table 1 but all the missing data are available in the literature.[24,27,33,35–37]

Results

Alkoxyamines **24dMe**, **24dPh** and **24g** were prepared using the atom transfer radical addition (ATRA) procedure[36,38] (Scheme 2). Alkoxyamine **24v** was prepared by 1,2-addition of **24s** onto *n*-butyl acrylate.[39] Alkoxyamine **24u** was obtained by hydrolysis of **24fMe**[34] according to a procedure previously described.[36]

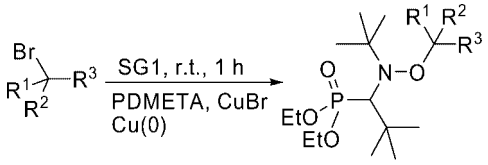

24

24dPh: $R^1 = R^2 = Me$, $R^3 = COOPh$
24dMe: $R^1 = R^2 = Me$, $R^3 = COOMe$
24g : $R^1 = R^2 = Me$, $R^3 = CN$

Scheme 2.

Kinetic measurements were performed by monitoring the decay of alkoxyamine concentration by means of ^{31}P NMR spectroscopy in the presence of an excess of thiophenol as alkyl radical scavenger.[40] Rate constants k_d are given by Equation (1).

$$\ln([\text{alkoxyamine}]/[\text{alkoxyamine}]_0) = -k_d \cdot t \quad (1)$$

All experiments were carried out twice and activation energies E_a were estimated using the averaged frequency factor (2.4×10^{14} s^{-1}) defined in the literature and all rate constants k_d were reestimated at 120 °C to be consistent with the literature.[24,27] The values of the radical stabilization constant σ_{RS},[33] the universal electrical (polar inductive/field) Hammett constant σ_I,[41,42] the Charton steric con-

Table 1. Activation energies E_a, rate constants k_d at 120 °C, radical stabilization Hammett constants σ_{RS}, universal electrical (polar inductive/field) Hammett constants σ_I, Charton steric constants υ, radical stabilization energies (RSE) and bond dissociation energies (BDE) of the new released alkyl radicals.

Alkoxyamine[a]	E_a[b]	k_d[c]	σ_{RS}[d]	σ_I[d]	υ[d]	RSE[b,d]	BDE(C–H)[b,d]	Ref.
24dPh	104.8[e]	2.82	0.20[f]	0.10[g,h]	1.35[i,j]	–11.7[f]	379.0(±15.0)[f]	this work
24g	107.3[k]	1.31	0.22	0.14	1.20	–14.2	362.6(±8.4)	this work
24dMe	108.9[l]	0.80	0.20	0.07	1.43	–11.7	379.0(±15.0)	this work
24d*s*Bu	110.3[m]	0.52	0.20[f]	0.07[g,n]	1.38[i,o]	–11.7[f]	379.0(±15.0)[f]	[37]
24s	112.3[p]	0.34	0.21	0.07	1.24	–12.3	388.5(±12.1)	[33]
24d*t*Bu	112.3[m]	0.28	0.20[f]	0.07[g,q]	1.37[i,r]	–11.7[f]	379.0(±15.0)[f]	[37]
24v	124.5[s]	6.80×10^{-3}	0.18[t]	0.10[u]	1.20[v]	–11.7[t]	385.0(±15.0)[t]	this work
24q	139.7[w]	6.50×10^{-5}	0.12	–0.01	1.24	0.0	404.0(±1.7)	[34]
24u	150.6[x]	2.30×10^{-6}	0.15[y]	0.11[z]	0.65	–12.3	407.5(±15.0)[aa]	this work

[a] SG1 as nitroxyl moiety. [b] In kJ/mol. [c] In s^{-1}. Values estimated using the E_a values in the second column and the average frequency factor A of 2.4×10^{14} s^{-1} given in refs.[24,27,29]. [d] Values given in ref.[33] unless otherwise mentioned. [e] Two runs, T = 25–30 °C. [f] See text. [g] Given by Equation (10). [h] $\sigma_{I,Ph} = 0.12$, see ref.[42]. [i] Given by Equation (11). [j] $\upsilon_{Ph} = 1.36$, see ref.[48]. [k] Three runs, T = 40–53 °C. [l] Three runs, T = 44–57 °C. [m] See ref.[37]. For **24d*t*Bu**, three runs, T = 52 –73 °C. [n] $\sigma_{I,sBu} = -0.01$, see ref.[42]. [o] $\upsilon_{sBu} = 1.02$, see ref.[43]. [p] See ref.[33]. [q] $\sigma_{I,tBu} = -0.01$, see ref.[42]. [r] $\upsilon_{tBu} = 1.24$, see ref.[43]. [s] Two runs at 81 °C. [t] Values estimated for the **eMe** fragment, see ref.[33]. [u] Given by Equation (3), $\sigma_{I,s} = 0.07$, $\sigma_{I,COOnBu} = \sigma_{I,COOMe} = 0.32$, see ref.[42]. [v] Given by Equation (5), $\upsilon_1 = \upsilon_{iPr} = 0.76$, $\upsilon_2 = \upsilon_{COOMe} = 0.9$, $\upsilon_3 = \upsilon_{Et} = 0.56$, see text and ref.[43]. [w] See ref.[34]. [x] Two runs at 150 °C. [y] Given by Equation (7). [z] Given by Equation (2), $\sigma_{I,COOH} = 0.30$, see ref.[42]. [aa] Given in ref.[45].

stant υ,[43] Rüchardt's radical stabilization energy (RSE),[44] the bond dissociation energy (BDE) of the C–H bond of the released alkyl radical,[45] k_d and E_a for the new alkoxyamines **24g**, **24dMe**, **24dPh**, **24u** and **24v** are listed in Table 1. All the data used in this work but not reported in this paper are available in the literature.[24,27,33–37] For convenience, the E_a values for the alkoxyamines not reported in Table 1 were also re-estimated using the mean frequency factor of 2.4×10^{14} s^{-1}.

The missing constants σ_I are given by Equations (2), (3) and (4) for primary, secondary and tertiary alkyl groups, respectively.[46] The missing constants υ are given by Equation (5), which is derived from the segmental approach of the steric effect by Charton.[47] In fact, with alkoxyamines, the first or basic fragment υ_1 is either *t*Bu, *i*Pr or Et for the tertiary, secondary and primary released alkyl radical, respectively. The values of υ_2 and υ_3 depend on the size of the groups, that is, $\upsilon_2 > \upsilon_3$. υ_3 is used only when one of the methyl groups is replaced by another group. The value of υ_3 was chosen in accordance with the minimal steric interaction (MSI) principle.[47] For example, with **24**-CH(COOMe)-CH_2CMe_2COOH, the alkyl fragment is CH(COOMe)-CH_2CMe_2COOH; thus υ_1 was *i*Pr, υ_2 was COOMe and υ_3 was Et because the bulky CH_2CMe_2COOH group presents its smallest hydrogen atoms to the reactive center (MSI principle) and thus should not be sterically more demanding than an ethyl group. The missing σ_{RS} constants are given by Equations (6) and (7) and it was assumed that the substituent of the ester group did not exert significant influence on the stabilization of the radical center.[33,35] It was also assumed that the radical $^{\cdot}CH(COO\mathit{n}Bu)CH_2CMe_2$-COOH exhibited the same radical stabilization effect as the radical $^{\cdot}$CHMeCOOMe.

$$\sigma_{I,R1CH2} = 0.416\sigma_{I,R1} - 0.0103 \quad (2)$$

$$\sigma_{I,R1R2CH} = 0.297\Sigma\sigma_{I,R} + 0.00482 \quad (3)$$

$$\sigma_{I,R1R2R3C} = 0.248\Sigma\sigma_{I,R} + 0.00398 \quad (4)$$

$$\upsilon = 0.866\upsilon_1 + 0.436\upsilon_2 + 0.348\upsilon_3 - 0.0455 \quad (5)$$

$$RSE^{corr}(primary)\ kJmol^{-1} = RSE - 9.6\ kJmol^{-1} \quad (6)$$

$$\sigma_{RS} = \frac{RSE^{corr}\ kJmol^{-1}}{\Delta H_f(CH_3^{\cdot})} \quad (7)$$

It has recently been shown that $\sigma_{I,\mathbf{CHMeCOOR}}$ and $\upsilon_{\mathbf{CHMeCOOR}}$ for the **eR** group are given by Equations (8) and (9).[48] The values of 0.3, 3.5 and 10 for the ratios of $k_{d,(\mathbf{24d\mathit{t}Bu})}/k_{d,(\mathbf{24deMe})}$, $k_{d,(\mathbf{24dPh})}/k_{d,(\mathbf{24dMe})}$ and $k_{d,(\mathbf{24dPh})}/k_{d,(\mathbf{24d\mathit{t}Bu})}$, respectively, are very similar to the corresponding ratios obtained with **24eR** (0.3, 2 and 6, respectively).[36,37] Thus, the effects observed with the isomers of the **24eR** series also occur with the tertiary **24dR** series. Consequently, $\sigma_{I,\mathbf{CMe2COOR}}$ and $\upsilon_{\mathbf{CMe2COOR}}$ should be given by Equations (10) and (11) with values of 0.267 and –0.099 for κ and ξ, respectively.

$$\sigma_{I,CHMeCOOR} = \sigma_{I,CHMeCOOMe} + \kappa\sigma_{I,R} - \kappa\sigma_{Me} \quad (8)$$

$$\upsilon_{CHMeCOOR} = \upsilon_{CHMeCOOMe} + \xi\upsilon_R - \xi\upsilon_{Me} \quad (9)$$

$$\sigma_{I,CMe2COOR} = \sigma_{I,CMe2COOMe} + \kappa\sigma_{I,R} - \kappa\sigma_{Me} \quad (10)$$

$$\upsilon_{CMe2COOR} = \upsilon_{CMe2COOMe} + \xi\upsilon_R - \xi\upsilon_{Me} \quad (11)$$

X-ray[49] crystallographic analysis of **24dPh**, **24s**, (*RR*/*SS*)- and (*RS*/*SR*)-**17** and (*RS*/*SR*)-**24eMe** provided geo-

Table 2. Significant lengths *l*, distances *d*, valence angles *a* and torsion angles θ for the X-ray structures of **24dPh**, **24s**, **17** [(*RR*/*SS*) and (*RS*/*SR*) diastereoisomers] and (*RS*/*SR*)-**24eMe** and for DFT-calculated structures of **24eMe** [(*RR*/*SS*) and (*RS*/*SR*) diastereoisomers] and **2** [(*RR*/*SS*) and (*RS*/*SR*) diastereoisomers].

	24dPh	**24s**	**17** (*RR*/*SS*)	**17** (*RS*/*SR*)	**24eMe** (*RS*/*SR*)	**24eMe** (*RS*/*SR*)[a]	**24eMe** (*RR*/*SS*)[a]	**2** (*RS*/*SR*)[a]	**2** (*RR*/*SS*)[a]
l [Å]									
O5–C6	1.460	1.463	1.429	1.438	1.433	1.434	1.435	1.435	1.435
N4–O5	1.458	1.458	1.467	1.457	1.454	1.450	1.454	1.450	1.454
C3–P2	1.856	1.854	1.851	1.840	1.843	1.883	1.885	1.883	1.885
P2–O1	1.457	1.466	1.456	1.469	1.460	1.492	1.491	1.492	1.492
O8–C9	1.416	–[b]	1.399	1.408	1.446	1.437	1.440	1.478	1.481
d [Å]									
N4–C6	2.497	2.508	2.411	2.368	2.409	2.428	2.420	2.429	2.420
O1–C7	5.356	5.246	5.161	2.881	3.921	3.972	5.265	3.987	5.271
a [°]									
<N4O5C6>	117.6	118.3	112.7	109.7	113.3	114.7	113.8	114.7	113.7
<C3N4O5>	106.1	109.1	106.1	108.5	107.8	105.6	107.0	108.5	107.0
<C7O8R>	118.3	109.5	118.1	116.3	116.3	115.5	115.4	122.1	122.1
θ [°]									
<O5C6C7O8>	35.1[c]	38.3[c]	39.8	28.0	28.6	25.2	40.5	25.9	38.1
<N4O5C6H>	6.7	7.9	9.2	45.4	72.7	75.7	6.5	76.6	5.9
$<C6O5N4n_{\sigma,N4}>$[d]	–13.1	–15.5	–6.6	20.9	13.5	12.7	–5.8	12.4	–5.4
<O1P2C3N4>	95.0	93.1	87.7	64.9	81.10	82.8	92.0	83.0	92.2
<C7C6O5N4>	117.0	115.3	111.3	162.6	169.8	169.0	113.6	169.1	114.4

[a] DFT-calculated geometric parameters. [b] Hydrogen atom instead of alkyl group. [c] <O5C6C7O10> values. The *anti* conformation for the O5C6C7O10 sequence is preferred, see text. [d] $<C6O5N4n_{\sigma,N_4}> = <C6O5N4C12> - 120°$.

metric data such as bond lengths *l*, interatomic distances *d*, valence angles α and torsion angles θ (Table 2), which, in general, are related to the effects ruling the C–ON bond homolysis of alkoxyamines (vide infra). It also provided information concerning the conformation of each molecule in the crystal state which are expected to be similar to the conformations in solution (Figure 3). Unfortunately, despite many attempts, it was not possible to grow crystals of the (*RR*/*SS*) diastereoisomers of **24eMe** and **2**. Thus, DFT calculations at the B3LYP/6-31G(d) level of theory were performed to determine the geometric parameters of the most stable conformers of the two diastereoisomers of **24eMe** and **2** (Figure 3). The calculated geometric parameters for the (*RR*/*SS*) diastereoisomer of **24eMe** agree well with the X-ray data (Table 2) and, thus, the data obtained by DFT calculations for the (*RR*/*SS*) diastereoisomers of **24eMe** and **2** and for the (*RS*/*SR*) diastereoisomer of **2** are assumed to be as reliable as those obtained by X-ray analysis. Furthermore, the calculated conformational structures of the (*RR*/*SS*) diastereoisomers of **24eMe** and **2**, and of the (*RS*/*SR*) diastereoisomer of **2** are very similar to those determined by X-ray analysis of the (*RR*/*SS*) diastereoisomer of **17** and the (*RS*/*SR*) diastereoisomers of **17** and **24eMe**, respectively. The X-ray data and calculations show that the nitrogen lone pair and the alkyl fragment of the alkoxyamines adopt the expected *syn* conformation (Figure 3 and Figure 4).[50] This conformation minimizes the repelling interactions between the nitrogen and oxygen lone pairs and the steric demand and although the alkyl fragment is in the same hemisphere as the bulky *t*Bu group it nearly eclipses the nitrogen lone pair (Figure 4). Owing to the absence of electrostatic interactions between the P=O and C=O groups (vide infra) in **24dPh**, **24s** and the (*RR*/*SS*) diastereoisomers of **24eMe**, **2** and **17** (Figure 4, Table 2), the alkyl group is slightly shifted to a position opposite the *t*Bu group, whereas for the (*RS*/*SR*) diastereoisomers of **24eMe**, **2** and **17**, in which P=O···C=O electrostatic interactions are likely to occur, the alkyl group is strongly shifted towards the *t*Bu group: 13.5°, 12.4° and 20.9° for the $<$C6O5N4$n_{\sigma,N4}>$ angle from the nitrogen lone pair, respectively (Table 2 and Figure 3). Such electrostatic interactions overbalance the repulsive electrostatic interaction between the n_p lone pair of the oxygen atom O5 and the n_σ lone pair of the nitrogen atom. Note that for **24dPh** and **24s** one of the methyl groups (shifted by a few degrees towards the *t*Bu group, Table 2, Figure 3 and Figure 5) nearly eclipses the nitrogen lone pair, which relieves the steric hindrance and moves the ester or acid group towards the least sterically and electrically demanding position. The same is observed for the hydrogen atom on C6 in the (*RR*/*SS*) diastereoisomers of **17**, **24eMe** and **2**, whereas the staggered form is preferred for their (*RS*/*SR*) diastereoisomers (Figure 3 and Figure 5, and $<$N4O5C6H$>$ in Table 2) because of the electrostatic interaction mentioned above.

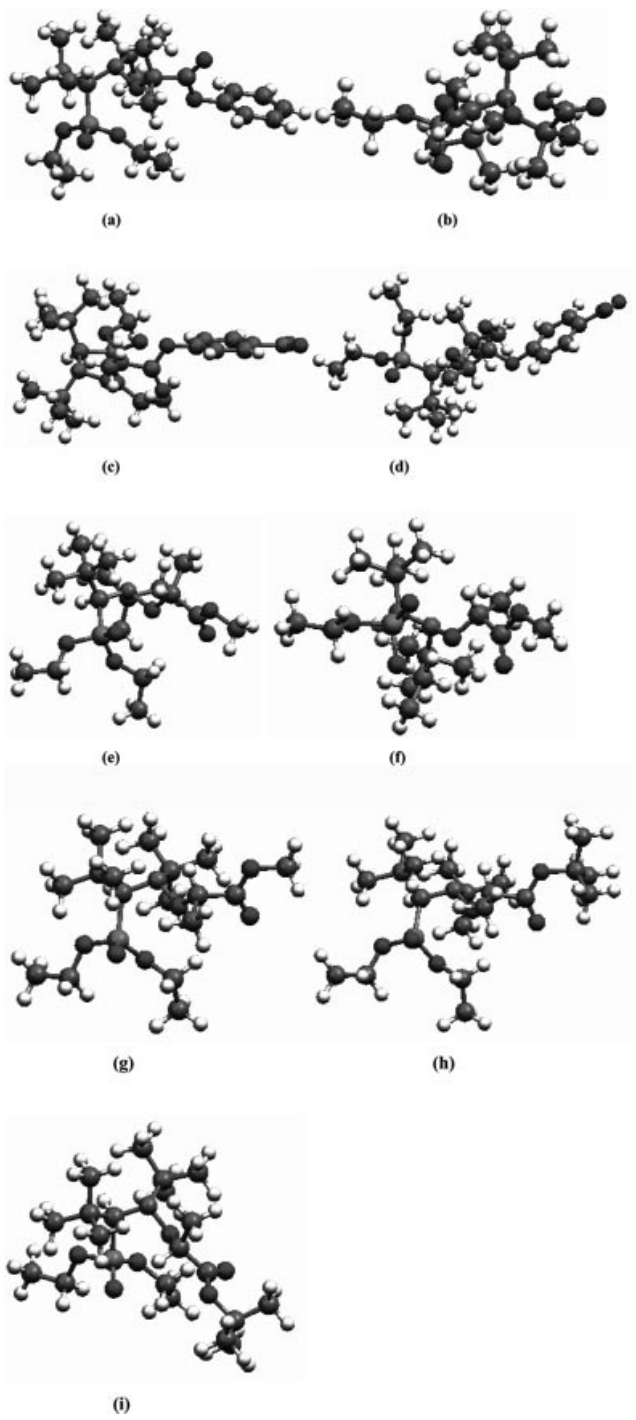

Figure 3. X-ray structures of (a) **24dPh**, (b) **24s**, (c) (*RR*/*SS*)-**17**, (d) (*RS*/*SR*)-**17** and (e) (*RR*/*SS*)-**24eMe**, and calculated structures of (f) (*RS*/*SR*)-**24eMe**), (g) (*RR*/*SS*)-**24eMe**, (h) (*RR*/*SS*)-**2** and (i) (*RS*/*SR*)-**2**.

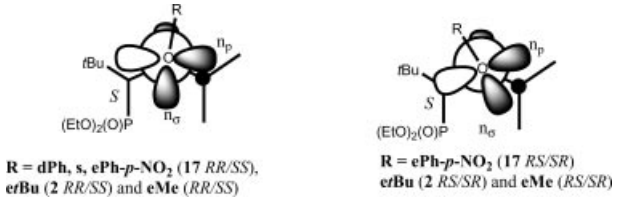

Figure 4. Newman projections along the N–O bond for the conformations given by X-ray analysis.

24dPh : R = Me and R^1 = Ph
24s : R = Me, R^1 = H
17 (*RR/SS*) : R = H and R^1 = Ph-*p*-NO_2
24eMe (*RR/SS*) : R = H and R^1 = Me
2 (*RR/SS*) : R = H and R^1 = *t*Bu

17 (*RS/SR*) : R^1 = Ph-*p*-NO_2
24eMe (*RS/SR*) : R^1 = Me
2 (*RS/SR*) : R^1 = *t*Bu

Figure 5. Newman projections along the C6···N atoms for the conformations given by X-ray analysis.

Because of steric hindrance and electrostatic interactions, the ester groups of the (*RS*/*SR*) diastereoisomers of **24eMe**, **2** and **17** are turned towards the phosphoryl group whereas in the other alkoxyamines they are opposite both the *t*Bu and phophoryl groups (Figure 3 and Figure 5, and <C7C6O5N4> in Table 2). Note that for **24dPh** and **24s**, which both carry a tertiary alkyl fragment, the relief of steric hindrance forces the cleaved O–C bond and the carbonyl group into the *anti* conformation whereas for the other molecules the *syn* conformation is preferred (Figure 3 and Table 2). For the alkoxyamine carrying an aromatic group, values of the <C7O8C9> angle of the ester function close to 120° (Table 2) show that the n_p lone pair of the oxygen atom is conjugated to the carbonyl function while the n_σ lone pair is conjugated to the aromatic ring (shortening of the O8–C9 bond length, Table 2). In addition, the carbonyl function is nearly orthogonal ($5° < \theta < 14°$) to the aromatic ring and, therefore, there is no conjugation between the carbonyl function and the aromatic ring (Figure 6).

24dPh : R = Me and R^1 = Ph
24s : R = Me and R^1 = H
17 (*RR/SS*) : R = H and R^1 = Ph-*p*-NO_2
24eMe (*RR/SS*) : R = H and R^1 = Me
2 (*RR/SS*) : R = H and R^1 = *t*Bu

17 (*RS/SR*) : R^1 = Ph-*p*-NO_2
24eMe (*RS/SR*) : R^1 = Me
2 (*RS/SR*) : R^1 = *t*Bu

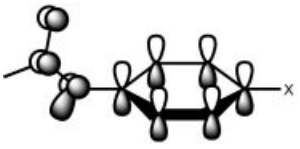

24dPh: X = H
17 : X = NO_2

Figure 6. Newman projections for the conformations of the alkyl groups, based on X-ray analysis.

Discussion

Methyl Effect

A few years ago, for the two triples (**a**, **b**, **c** and **d*t*Bu**, **e*t*Bu**, **f*t*Bu**) and a few pairs of TEMPO-based alkoxyamines,[24] it was shown that the introduction of one methyl group into the leaving radical on average decreased the value of E_a by 17 ± 4 kJ/mol. We recently showed that observations with TEMPO-alkoxyamines cannot be extended to SG1-based alkoxyamines, for example, the alkyl ester group exerts a steric effect in the SG1 series but not in the TEMPO series.[37,33,34] Nevertheless, for the three triples (**g**, **h**, **i**, **dMe**, **eMe**, **fMe** and **s**, **t**, **u**) a considerable methyl steric effect is evident, for example, E_a decreases by about 40 kJ/mol from **fR** to **dR** in both the TEMPO (R = *t*Bu) and SG1 (R = Me) series. It is important to note that the R group has no effect on the value of k_d for the TEMPO-based alkoxyamines and only the methyl ester is considered for SG1-based alkoxyamines.[37] Similarly, in the series **g**, **h**, **i** and **s**, **t**, **u**, by replacing a hydrogen atom by a methyl group, E_a decreases by 16.8 and 19.5 kJ/mol from the tertiary to secondary alkyl fragments, respectively, and by 13.1 and 18.8 kJ/mol from the secondary to primary alkyl fragments, respectively. That is, on average, the introduction of one methyl group into the leaving radical reduces E_a by 17 kJ/mol for the SG1 alkoxyamines. Thus, an increment of –(17 ± 5) kJ/mol for the introduction is estimated for all triples and pairs available with any nitroxyl fragment. In fact, out of the 22 values of ΔE_a available, only three are outside the error limits, that is, ΔE_a is more than 10 kJ/mol.

Because the ablility to predict the activation energies and thus the values of k_d is of great interest, the predictive scale proposed by Marque et al.[24] was extended to new released alkyl radicals. Because **b**-based alkoxyamines are the most studied, the **b** group was chosen as a benchmark and all alkyl fragments available, whatever the nitroxyl moiety, were scaled to it (Figure 7). For example, changing from **b** to **q** changes the activation energy of TEMPO derivatives by +12.9 kJ/mol, of SG1 derivatives by +14.5 kJ/mol, of TIPNO derivatives[51] by +16.6 kJ/mol (molecules **7a** and **7b** in ref.[27]) and by +15.0 kJ/mol (molecules **8b** and **8c** in ref.[27]) and of DBNO derivatives[51] by +15.5 kJ/mol. When several ΔE_a values were available, the average is reported in Figure 7.

l	**g**	**a**	**dR**	s	j	**b**
–53.5	–17.7	–16.4	–12.8	–12.9	–6.5	**0**
h	**n**	**m**	**eR**	**k**	**t**	**i**
+0.1	+1.2	+4.8	+6.3	+6.5	+6.6	+10.8
c	**q**	**u**	**fR**	**p**	**o**	**r**
+13.0	+14.8	+25.2	+26.2	+34.6	+44.0	+60.6 kJ/mol

Figure 7. Incremental scale for various alkyl fragment with group **b** as benchmark.

Bond Dissociation (BDE) and Radical Stabilization Energies (RSE)

It has recently been shown for TEMPO-based alkoxyamines that the E_a values are correlated to the BDE(C–H) of the released alkyl radical.[24,27] On the other hand,[33] for SG1-based alkoxyamines two correlations were observed, one for the primary and secondary nonpolar alkyl groups and another for the primary and secondary polar alkyl

groups. Furthermore, two other correlations were expected: one for the nonpolar and one for the polar tertiary alkyl groups.[33,34] Because tertiary groups **24q** and **24s** are shifted by about 20 kJ/mol from the nonpolar and polar lines, it was expected that the polar tertiary alkyl groups would exhibit a linear correlation with a slope similar to that of secondary and primary polar alkyl radicals [Equation (12)]. However, the slope observed [Equation (13)] is clearly different from what was expected (Figure 8). Because the multiparameter approach accounts well for tertiary alkyl radicals (vide infra), such a result is certainly due to large errors[45] in the BDE values (Table 1), for example, assuming values of 370, 373 and 376 kJ/mol for the BDE(C–H)s of **g-H**, **dR-H** and **s-H**, respectively (values given when the errors are accounted for, Table 1), the slope is in fact very similar to the expected value (not shown). Figure 8 reveals the importance of having accurate values of BDE(C–H) and the limits of this approach to provide accurate estimates of k_d. Note that the E_a value for **24u** lies close to the polar line. Thus, the deviating data for **24fMe** is probably due to the experimental conditions.[52]

$$E_a\ (\text{kJ/mol}) = -177.8(\pm 60.4) + 0.80(\pm 0.15) \times \text{BDE} \quad (12)$$
$$R^2 = 0.746;\ s = 5.2;\ N = 11$$

$$E_a\ (\text{kJ/mol}) = 40.7(\pm 25.7) + 0.18(\pm 0.07) \times \text{BDE} \quad (13)$$
$$R^2 = 0.878;\ s = 1.3;\ N = 3$$

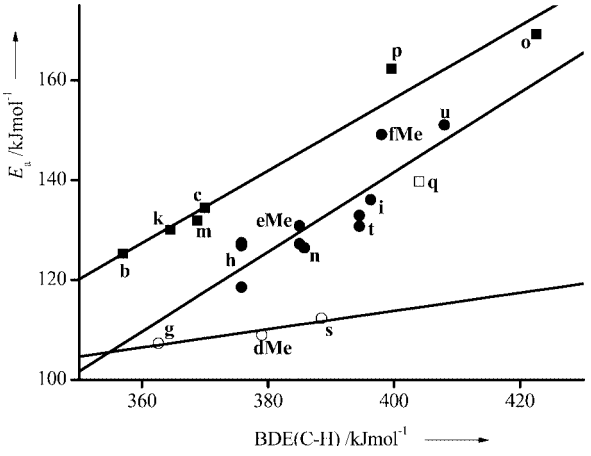

Figure 8. E_a versus BDE(C–H) for SG1-based alkoxyamines. Filled symbols: primary and secondary alkoxyamines; empty symbols: tertiary alkoxyamines; squares: nonpolar alkoxyamines; circles: polar alkoxyamines.

In a recent report of TEMPO-based alkoxyamines, a plot of E_a versus RSE highlighted the importance of the stabilizing effect of the released alkyl radical, whereas, the data for secondary and primary SG1-based alkoxyamines in such a plot is widely scattered (Figure 9).[33] However, the good correlation observed for the E_a values of tertiary alkyl radicals with RSE [Equation (14)] led us to re-analyze Figure 9. In fact, good correlations between E_a and RSE with similar slopes are observed only when **i**, **fR**, **u** and **o** [Equation (15)] and **h**, **eR**, **t** and **p** [Equation (16)] as primary and secondary alkyl radicals, respectively, are considered. Thus, SG1-based alkoxyamines with **b**, **k**, **m**, **c** and **n** are outliers. Figure 9 exemplifies the importance of both radical stabilization (three linear correlations) and the steric demand (outliers) of the alkyl fragment.

$$E_a\ (\text{kJ/mol}) = 139.4(\pm 2.4) + 2.4(\pm 0.2) \times \text{RSE} \quad (14)$$
$$R^2 = 0.982;\ s = 2.5;\ N = 4;\ t = 99.14\%$$

$$E_a\ (\text{kJ/mol}) = 170.2(\pm 5.6) + 2.0(\pm 0.5) \times \text{RSE} \quad (15)$$
$$R^2 = 0.884;\ s = 5.7;\ N = 4;\ t = 94.00\%.$$

$$E_a\ (\text{kJ/mol}) = 162.3(\pm 2.6) + 2.7(\pm 0.2) \times \text{RSE} \quad (16)$$
$$R^2 = 0.968;\ s = 2.6;\ N = 7;\ t = 99.99\%$$

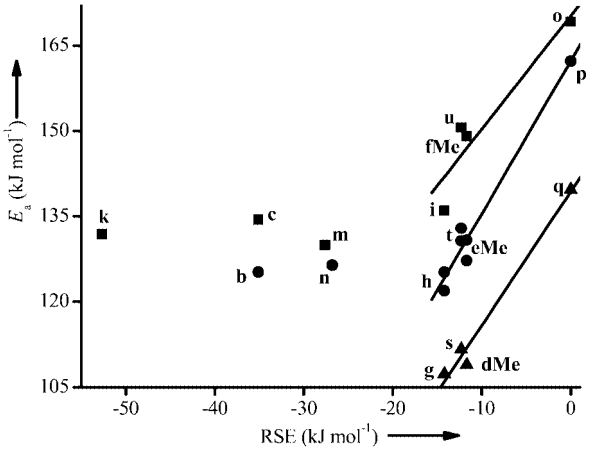

Figure 9. E_a versus RSE for SG1-based alkoxyamines. Squares: primary alkoxyamines; circles: secondary alkoxyamines; triangles: tertiary alkoxyamines.

Multiparameter Approach

We have recently shown that Equation (17) accounts for the stabilizing, steric and polar effects involved in the homolysis of the C–ON bonds of primary and secondary alkyl fragments of SG1-based alkoxyamines and of **24q** and **24s**.[33] As expected, **24u**, **24g** and **24dMe** lie on a straight line [see Figure 10 and Equation (S1) in the Supporting Information].

$$\log k_d = -14.04(\pm 0.83) + 14.30(\pm 1.41)\sigma_{RS} + 21.44(\pm 1.91)\sigma_I + 6.89(\pm 0.72)\upsilon \quad (17)$$
$$R^2 = 0.94;\ s = 0.48;\ F_{18,99.99\%} = 75$$

Recently, for the series **1**–**22** (Figure 1), we have shown that long-range polar and reverse steric effects occur.[35,48] The polar effect was described as a *normal* polar effect with the slower isomer [(*RR*/*SS*)] and as an *enhanced* polar effect (upward deviation) with the faster isomer [(*RS*/*SR*)]. Conversely, the faster isomer might display a *normal* polar effect and the slower one a *retarded* polar effect (downward deviation). Therefore, the linear regression [Equation (18) and Figure 11] observed for the primary alkoxyamines **24c**, **24i**, **24k**, **24p**, **24m** and **24u**, the nonpolar secondary alkoxyamines **24b** and **24o**, the tertiary alkoxyamines **24q**, **24s**, **24dMe** and **24g** and the secondary polar alkoxyamines **24t** and **24w** accounts for merely the *normal* polar effect assuming that the primary and tertiary fragments adopt the

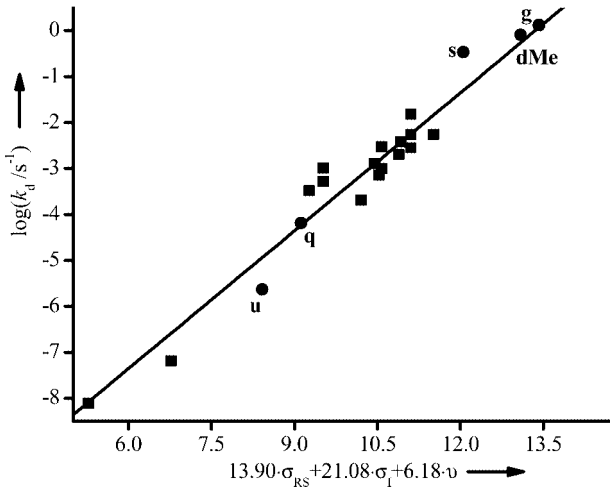

Figure 10. Log k_d for C–ON bond homolysis in SG1-based alkoxyamines versus a linear combination of molecular descriptors (σ_{RS}, σ_I and υ). Circles denote tertiary alkyl and new SG1-based alkoxyamines.

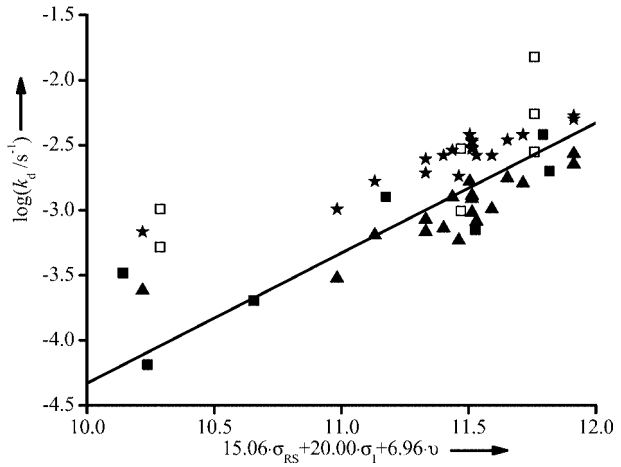

Figure 12. Log k_d for C–ON bond homolysis in SG1-based alkoxyamines versus a linear combination of molecular descriptors (σ_{RS}, σ_U and υ). (■): alkoxyamines of Equation (18); (□): polar secondary alkyl and the penultimate fragments; (★): the (*RR*/*SS*) isomer of **24eR**; (▲): the (*RS*/*SR*) isomer of **24eR**.

same conformation. When **24dtBu** and **24dPh** are also included in Figure 11, they lie on the straight line [Equation (18)], confirming that the *normal* polar effect occurs. Hence, for **24eMe**, **24h** and **24t**, which exhibit two isomers, the isomer that is closer to the straight line should exhibit the *normal* polar effect (Figure 11). The upward deviation observed for the faster isomers highlights the *enhanced* polar effect (Figure 11). For the series **1**–**22**, Figure 12 shows that the (*RR*/*SS*) isomers (the slower ones) of **24eR** are closer (*normal* polar effect) to the correlation [Equation (18)] and that the *enhanced* polar effect is emphasized by the upward deviation of the (*RS*/*SR*) isomer of **24eR**. Clear evidence and explanations about the polar effect have been given in previous papers.[33–35,48]

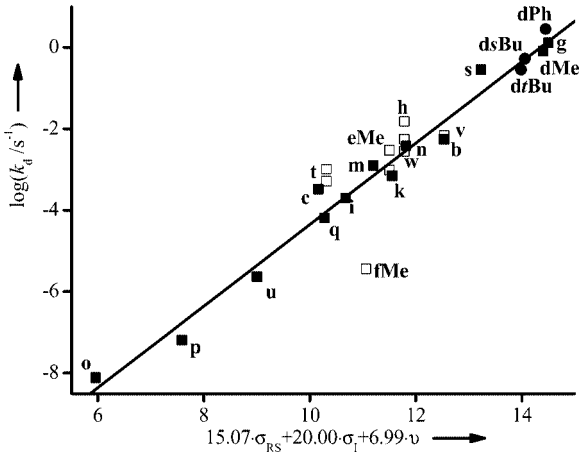

Figure 11. Log k_d for C–ON bond homolysis in SG1-based alkoxyamines versus a linear combination of molecular descriptors (σ_{RS}, σ_I and υ). (■): alkoxyamines of Equation (18); (●): alkoxyamines exhibiting long-range polar and steric effects; (□): polar secondary alkyl groups.

$$\log k_d = -14.33(\pm0.54) + 15.06(\pm1.17)\sigma_{RS} + 20.00(\pm1.86)\sigma_I + 6.96(\pm0.43)\upsilon \quad (18)$$
$$R^2 = 0.98;\ s = 0.41;\ F_{14,99.99\%} = 152$$

Note that the combination of Equations (3), (5) and (18) accounts for the stabilizing, polar and steric effects of the **v** fragment. Therefore, the multiparameter approach [taking into account 43 alkoxyamines, see Equation (S2) and Figure S1 in the Supporting Information] is versatile enough to predict the rate constant k_d when the penultimate effect is involved (Figure 11).[53]

X-ray Analysis and DFT Study

In their seminal paper, Moad and Rizzardo[15] pointed out that the lengthening of the cleaved C–ON bond and the opening of the <N4O5C6> angle are not the most suitable geometric parameters to correlate to the reactivity of alkoxyamines, whereas the increase in the C6···N4 distance encompasses both parameters and is more directly related to the ease of C–ON bond homolysis. Thus, on going from **24eMe** to **24s**, a 100–300-fold increase in k_d is observed whereas, unsurprisingly, a small Δl of 0.03 Å is measured. On the other hand, a clear increase of about 0.1 Å for Δd (N4···C6, Figure 3 and Table 2) and of about 5° for Δa (<N4O5C6>, Figure 3 and Table 2) is observed. The same behavior can be observed for alkoxyamines with aromatic groups. These two parameters are probes for steric hindrance, that is, an increase in *a* and *d* values with increasing steric hindrance is observed together with an increase in the value of k_d when replacing the hydrogen atom on the secondary alkyl fragment (**eR**) by the methyl group in the tertiary alkyl fragment (**s** or **dPh**). Also note that C3–P2 lengths increase by 0.011 Å on going from **24eMe** to **24s**. However, these four geometric parameters [*l*(O5–C6), *l*(P2–C3), *d*(N4···C6) and *a*(<N4O5C6>)] do not entirely account for the reactivity observed; that is, on going from **24s**

to **24dPh** a 10-fold increase in k_d is observed whereas no significant changes in the geometric parameters are observed, that is, Δl = –0.003 and 0.002 Å, Δd = –0.011 Å and Δa = –0.7°. Consequently, the correlations between geometric parameters and k_d values are poor and neither provide a clear insight into the effects involved in C–ON bond homolysis nor predict accurate values of k_d.

We recently mentioned that the *enhanced* polar effect may be due either to a peculiar conformation or to a through-space interaction between the P=O and C=O functions.[48] Therefore, the preferred conformations in alkoxyamines provided by X-ray data and calculations should help to discriminate between the structural effects involved in the homolysis step. For **24dPh**, **24s** and the (*RR*/*SS*) diastereoisomers of **17**, **2** and **24eMe**, the X-ray data and calculations (Figure 3 and Table 2) show that the distance between O1 and C7 is longer than 5 Å, that is, more than the sum of their van der Waals radii (r_O = 1.65 Å and r_C = 1.85 Å),[43] that the carbonyl function is insulated from the effect of the phosphoryl group by the presence of a methyl group in between and that the P=O function is turned away (open <O1P2C3N4> angle in Table 2) from the carbonyl function. Therefore, any electrostatic interactions between the partial negative charge δ^- on O1 and the partial positive charge δ^+ on C7 are discarded. Note that the only significant differences (Table 2) between the (*RR*/*SS*) diastereoisomers of **2** and **24eMe** are the 0.04 Å lengthening of *l*(O8–C9) and the 6.7° valence angle opening <C7O8C9>, which underlines a larger steric strain in **2** than in **24eMe**, which hampers the conformational changes required for homolysis to occur (vide infra). For the (*RS*/*SR*) diastereoisomers of **17**, **2** and **24eMe**, the X-ray data and calculations (Figure 3 and Table 2) show that the distances between O1 and C7 are 2.881, 3.987 and 3.972 Å, respectively, that is, smaller than or close to the sum of their van der Waals radii, that no methyl group insulates the carbonyl function from the phosphoryl group and that the P=O function is turned toward (close <O1P2C3N4> angle in Table 2) the carbonyl function. Therefore, electrostatic interactions may occur between the partial negative charge δ^- on O1 and the partial positive charge δ^+ on C7 (Figure 13). If such interactions were strong, they should modify the partial charges on P2, O1, C6, C7 and O10 and one would expect an increase in the partial positive charge on C7, which would increase the electronegativity χ of C6 and thus increase the value of k_d. The NBO charges obtained after DFT calculations on the two diastereoisomers of **24eMe** and **2** at the B3P86/6-311++G(d,p)//B3LYP/6-31G(d) level of theory show no difference in the partial charges of the two diastereoisomers (Table). Therefore, such an electrostatic interaction does not account for the difference in the values of k_d between the two diastereoisomers of **24eMe** and **17** which carries a strongly electron-withdrawing group (C_6H_5-*p*-NO_2) as ester substituent.[35] However, this electrostatic interaction is likely to play a role in the adoption of the preferred conformation.

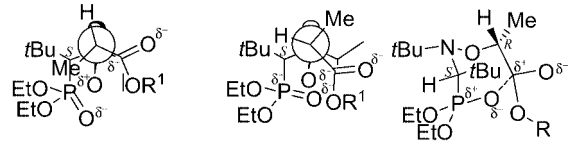

17 (*RR*/*SS*) : R^1 = Ph-*p*-NO_2
24eMe (*RR*/*SS*) : R^1 = Me
2 (*RR*/*SS*) : R^1 = *t*Bu

17 (*RS*/*SR*) : R^1 = Ph-*p*-NO_2
24eMe (*RS*/*SR*) : R^1 = Me
2 (*RS*/*SR*) : R^1 = *t*Bu

Figure 13. Conformational requirements for electrostatic interactions.

A detailed analysis of the conformations shows that the *anti* conformation for the O5–C6–C7–O10 sequence is adopted in **24dPh** and **24s** whereas the *syn* conformation is preferred for **24eMe**, **2** and **17** (Figure 14). Note that the (*RR*/*SS*) and (*RS*/*SR*) diastereoisomers of **24eMe**, **2** and **17** do not exhibit the same *syn* conformation (<O5C6C7O8> in Table 2), that is, the O5–C6 and C7–O8 moieties are staggered by roughly 30 and 40° in the (*RS*/*SR*) and (*RR*/*SS*) diastereoisomers, respectively (Figure 14). NBO analysis (Table 3) of the diastereoisomers of **24eMe** and **2** shows strong $n_p \rightarrow \pi$ interactions ($E \approx$ 200.0 kJ/mol) between the n_p lone pair of O8 and the π system of the carbonyl function for both alkoxyamines, as expected from the X-ray data. Furthermore, NBO analysis (Table 3) shows $n_\sigma \rightarrow \sigma^*$ overlapping ($E \approx$ 2.6 kJ/mol) between the n_σ lone pair of O8 and the σ* orbital of the cleaved O–C bond of the (*RS*/*SR*) diastereoisomers of both **24eMe** (Figure 15) and **2** while this type of overlapping ($E <$ 2 kJ/mol) is not observed for the (*RR*/*SS*) diastereoisomer of **24eMe** and is weak (E ≈ 2 kJ/mol) for the (*RR*/*SS*) diastereoisomer of **2** (Figure 14). Thus, for the (*RS*/*SR*) diastereoisomer, popu-

Table 3. NBO charges and interaction energies for the (*RR*/*SS*) and (*SR*/*RS*) diastereoisomers of **24eMe** and **2**.[a]

		24eMe (*RS*/*SR*)	(*RR*/*SS*)	**2** (*RS*/*SR*)	(*RR*/*SS*)
NBO charges[b]	O1	–1.08	–1.08	–1.08	–1.08
	P2	2.33	2.33	2.33	2.33
	O5	–0.48	–0.48	–0.48	–0.48
	C6	0.04	0.04	0.04	0.04
	C7	0.81	0.80	0.82	0.82
	O10	–0.60	–0.61	–0.61	–0.62
Interaction energies[c]	$n_{\sigma,O8} \rightarrow \sigma^*_{C6-O5}$	2.6	<2.0	3.0	2.2
	$n_{p,O8} \rightarrow \pi_{C7=O10}$	199.8	203.1	206.2	210.3

[a] Structures of the (*RR*/*SS*) and (*RS*/*SR*) diastereoisomers of SG1 **24eMe** and **2** were calculated at the B3LYP/6-31G(d) level of theory. The single point energies were then calculated at the B3P86/6-311++G(d,p) level of theory. [b] Given in a.u. [c] In kJ/mol.

lating the σ* orbital of the O6–C7 bond with electrons from the O8 lone pair weakens the O6–C7 bond and consequently increases the value of k_d. This type of overlapping does not stabilize the transition state (TS) because, here, the favoured orbital overlappings are between the n_p lone pair of the O8 atom and the π bond of the carbonyl function, and between the σ* orbital of the cleaved C–O bond and the π bond of the carbonyl function, excluding any $n_\sigma \rightarrow \sigma^*$ overlapping (n_σ is nearly orthogonal to σ*, Figure 16) as described in Figure 14. On the other hand, the increase of about 15 and 12° in the <O5C6C7O8> torsion angle in the (*RR*/*SS*) diastereoisomers of **24eMe** and **2**, respectively (Table 2), suppresses this $n_\sigma \rightarrow \sigma^*$ orbital overlapping and the *normal* polar effect is observed, as in the case of **24s** and **24dPh** in which the *anti* conformation forbids such $n_\sigma \rightarrow \sigma^*$ overlapping. Moreover, such $n_\sigma \rightarrow \sigma^*$ orbital overlapping is dependent on the electron-donating capacity of the oxygen lone pair, that is, the presence of a strongly electron-withdrawing group such as a halogen atom or a *p*-nitroaromatic group on the ester moiety should reduce the capacity of the oxygen atom to share its lone pair and then weaken the $n_\sigma \rightarrow \sigma^*$ orbital overlapping. Hence, the *enhanced* polar effect decreases with increasing polarity of the ester fragments, as observed with the aromatic and halogenated derivatives **10**–**17** and **18**–**22**, respectively, that is, a smaller slope for the polar effect is observed with the (*RS*/*SR*) diastereoisomers of **10**–**22** than for the (*RR*/*SS*) diastereoisomers of **10**–**22**.[35]

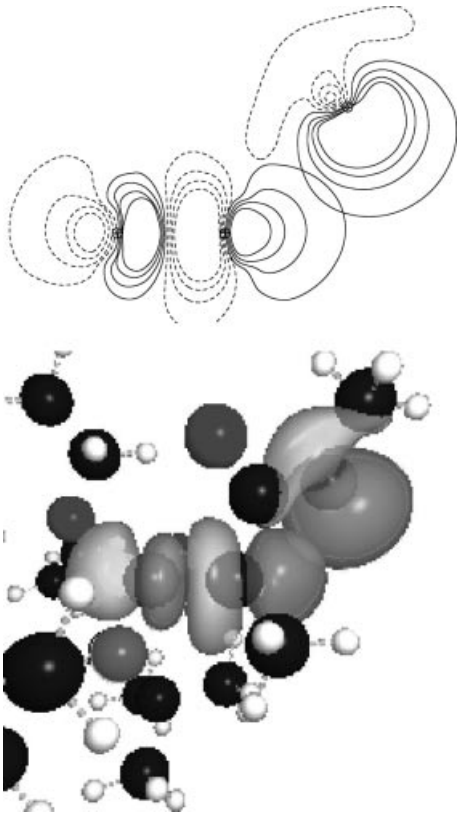

Figure 15. NBO plots for the $n_{\sigma,O8} \rightarrow \sigma^*_{O5-C6}$ interaction in the (*RS*/*SR*) diastereoisomer of **24eMe**.

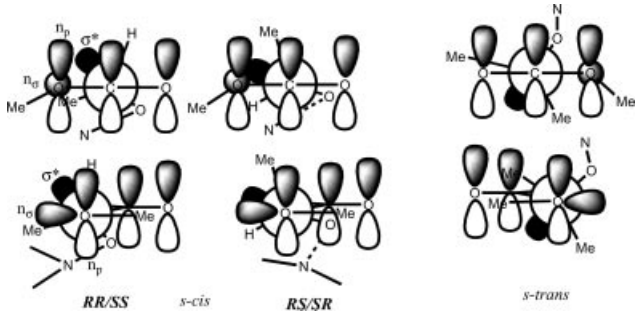

Figure 14. Conformational requirements for the $n_O \rightarrow \sigma^*_{O-C}$ interaction.

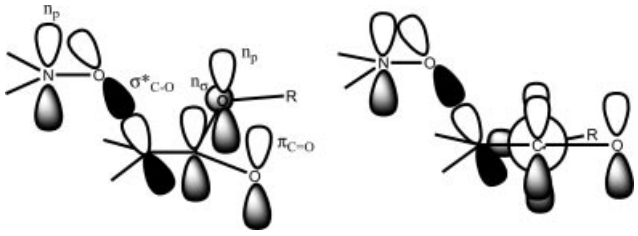

Figure 16. Orbital overlapping requirements for the TS of C–ON bond homolysis.

The absence of the *enhanced* polar effect for aromatic, vinyl and keto groups is probably caused by conformations that forbid $\pi \rightarrow \sigma^*$ interactions and its absence for alkyl groups is evidently caused by the absence of both π systems and heteroatoms for which $\pi \rightarrow \sigma^*$ and $n_\sigma \rightarrow \sigma^*$ interactions may occur, respectively.

It should be mentioned that the $n_p \rightarrow \pi$ interaction is stronger for the (*RR*/*SS*) than for the (*RS*/*SR*) diastereoisomers of both **2** and **24eMe** (Table 3). Thus, it can be assumed that the stronger the interaction is, the more stabilized the (*RR*/*SS*) diastereoisomer is, and thus the lower k_d is. However, the absence of changes in <C7O8C9> and l_{O8-C9} indicates that such an interaction does not affect the value of k_d and thus should be disregarded as an explanation for the differences in the reactivity of the (*RR*/*SS*) and (*RS*/*SR*) diastereoisomers.

Homolysis Pathway

By virtue of the Hammond postulate, for an endothermic reaction (late TS) the structure of the activated complex at the transition state (TS) strongly resembles the structures of the products, that is, the structures of the nitroxyl and alkyl radicals. Recent X-ray studies[54,55] on SG1-type nitroxyl radicals **A**˙ and **B**˙ (Figure 17) have shown that the alkyl groups flanking the nitroxyl function adopt the eclipsed-conformation and that the nitroxyl function is in a staggered conformation with both alkyl groups (Figure 18, a).

Consequently, the same conformation is expected in the TS with the nitrogen atom flattened. Furthermore, homolysis requires $n_{p,N} \rightarrow \sigma^*_{O-C}$ and $\sigma^*_{O-C} \rightarrow \pi_{COOR}$ interactions leading to the expected arrangement in the TS displayed in Figure 18 (b). On the other hand, all the X-ray structures displayed in this work (Figure 3) show only one methyl group attached to the C6 atom facing the alkyl fragment. This means that in contrast to the nitroxyl radical, the nitroxyl fragment prefers the staggered/eclipsed conformation, as displayed in Figure 18c. Furthermore, the ester group of the alkyl fragment adopts a conformation in which the π orbital is turned 90° from the position required in the TS, as displayed in Figure 18 (c). Thus, this leaves us with two possible pathways for C–ON bond homolysis. The first commonly accepted pathway exhibits one TS. In this case, homolysis involves a strong activation entropy $\Delta S^{\ddagger}$ effect composed of at least four events: nitrogen flattening, transition from sp^3 to sp^2 hybridization for C6, restricted C6–C7 bond rotation (long-range steric effect), restricted C12–N bond rotation (the structure of the intermediate displayed in Figure 18 (d) is not the most stable although it resembles very much the TS), and probably a few other minor rotations. The clear difference between the conformations of the nitroxyl fragment (Figure 18, c) and the nitroxyl radical (Figure 18, a) leads us to invoke a pathway for homolysis that involves an intermediate (Figure 18, d) and two TSs (Figure 19). Hence, homolysis of the C–ON bond would proceed (Scheme 3) starting from the alkoxyamine in the *syn* conformation (Figure 3, Figure 4 and Figure 18, c) towards the intermediate displayed in Figure 18 (d), and then through TS2, which exhibits the requirements mentioned earlier (Figure 18, b), to yield the nitroxyl and alkyl radicals. Preliminary results[56,57] support a change of mechanism that would involve the intermediate displayed in Figure 18 (d). For a deeper insight into the homolysis pathways, kinetic studies[58] and calculations are underway. However, the pathway involving two TSs might hold only for alkoxyamines related to the SG1 family.

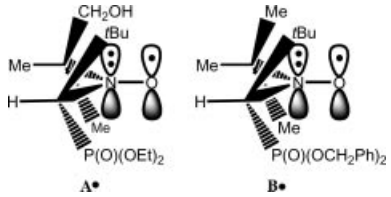

Figure 17. Eclipsed/staggered conformation of two SG1-type nitroxyl radicals.

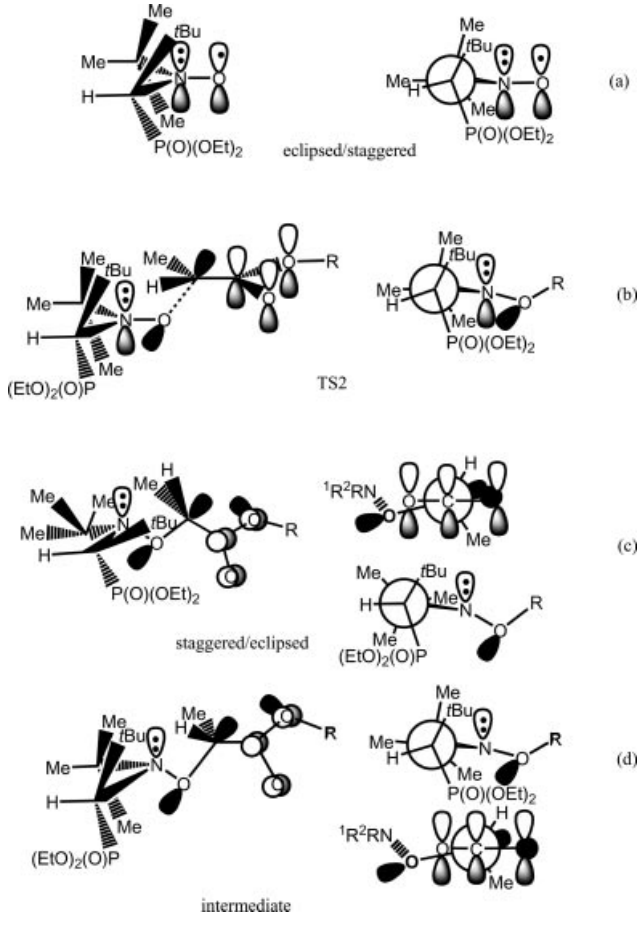

Figure 18. Newman projections, conformational requirements, orbital overlappings and structures of (a) the nitroxyl radical SG1, (b) TS2, (c) the alkoxyamine and (d) the intermediate.

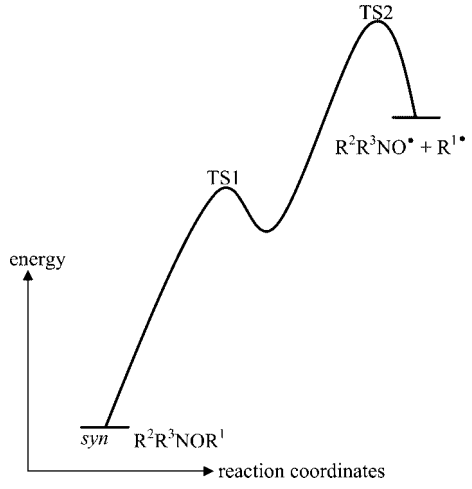

Figure 19. Homolysis pathway involving an intermediate.

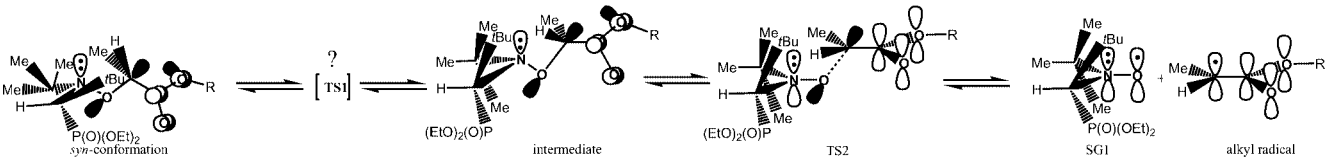

Scheme 3.

Conclusions

Rate constants k_d for the homolysis of the C–ON bond of alkoxyamines can be estimated either roughly with the scale given in Figure 7 or accurately with Equations (17) and (S1). Furthermore, stabilizing, *normal* polar, steric and penultimate effects are very well accounted for by Equations (17) and (S1). In addition to the steric, reverse steric, stabilizing and polar effects, the stereoelectronic effect, that is, $n_\sigma \rightarrow \sigma^*$ orbital overlapping, also affects C–ON bond homolysis, that is, k_d increases. The combination of Equations (17) and (8) developed by Marque[29] should become a powerful tool in the design of new alkoxyamines as well as in the analysis of k_d values.

Experimental Section

Solvents for synthesis, copper bromide, copper metal, *N*,*N*,*N*′,*N*′,*N*′′-pentamethyldiethylenetriamine (PMDETA), 2-bromo-2-methylpropionic acid methyl ester, 2-bromo-2-methylpropionyl bromide and bromoacetic acid were purchased from Aldrich and used as received. TEMPO was purchased from ACROS and sublimed. *tert*-butylbenzene was purchased from Aldrich and purified by conventional procedures.[59] Nitroxyl radical SG1 was kindly provided by ARKEMA. NMR experiments were performed with a 300 Avance Bruker spectrometer (^{1}H: 300 MHz; ^{13}C: 75.48 MHz; ^{31}P: 121.59 MHz) at the "Spectropole in Marseille". Chemical shifts were measured relative to TMS (internal reference) for ^{1}H NMR, to $CDCl_3$ (internal reference) for ^{13}C NMR and to 85% H_3PO_4 (external reference) for ^{31}P NMR spectroscopy. Elemental analyses were performed at the "Service Commun de Micro Analyse, Université Aix-Marseille 3". Reactions were monitored by TLC (60 F 240 silica gel plates; eluent: ethyl acetate/pentane 1:1), UV and phosphomolybdic acid being used as indicators. Alkoxyamines were purified by chromatography (60 silica gel, 70–230 mesh, Merck; eluent: ethyl acetate/pentane, 3:1). 2-Bromo-2-methylpropionic acid phenyl ester[60] and 2-bromo-2-methylpropionitrile[61] were prepared from 2-bromo-2-methylpropionyl bromide and acrylonitrile, respectively, as described in the literature. **24u** was prepared by hydrolizing **24fMe** according to the procedure previously described.[36]

General Procedure (GP): PMDETA (4.3 mL, 20.4 mmol) was added to a degassed solution of CuBr (1.47 g, 10.2 mmol) and copper (0.65 g, 10.2 mmol) in benzene, and nitrogen was bubbled through the solution for 10 min. A degassed benzene solution of SG1 (2.0 g, 6.8 mmol) and alkyl bromide (1.5 equiv.) was transferred to the mixture which was then stirred for 1 h at room temp. under nitrogen. Diethyl ether (30 mL) was added and the solid filtered off. The organic layer was washed with water until colorless and then dried with $MgSO_4$. The solvent was removed to yield an oil which was purified by silica gel column chromatography when needed.

Methyl 2-Methyl-2-[*N*-*tert*-butyl-*N*-(1-diethoxyphosphoryl-2,2-dimethylpropyl)aminoxy]propionate (24dMe): Compound **24dMe** (2.15 g, 5.44 mmol, 80%) was obtained as a white solid after allowing 2-bromo-2-methylpropionic acid methyl ester (1.85 g, 10.2 mmol) and SG1 (2 g, 6.8 mmol) in benzene (20 mL) to react with CuBr (1.47 g, 10.2 mmol), Cu^0 (0.65 g, 10.2 mmol) and PMDETA (3.52 g, 20.4 mmol) in benzene (20 mL) for 0.5 h at room temp. After drying under high vacuum (6×10^{-2} mbar) no further purification of **24dMe** was needed. ^{1}H NMR: δ = 4.39–4.28 (m, 2 H, CH_2), 4.10–3.90 (m, 2 H, CH_2), 3.70 (s, 3 H, OCH_3), 3.28 (d, $^2J_{H,P}$ = 27 Hz, 1 H, CHP), 1.67 (s, 3 H, CH_3), 1.61 (s, 3 H, CH_3), 1.38–1.27 (m, 6 H, CH_3), 1.17 (s, 9 H, *t*Bu), 1.10 (s, 9 H, *t*Bu) ppm. ^{13}C NMR: δ = 175.72 (C=O), 83.57 (OC), 70.23 [d, $^1J_{C,P}$ = 136.6 Hz, CH], 62.23 (CN), 61.84 (d, $^2J_{C,P}$ = 6.04 Hz, CH_2), 59.08 (d, $^2J_{C,P}$ = 7.54 Hz, CH_2), 51.85 (s, OCH_3), 36.04 (d, $^2J_{C,P}$ = 6.0 Hz, PC*C*), 29.93 [d, $^3J_{C,P}$ = 5.28 Hz, PCC(CH_3)$_3$], 28.25 [NC(CH_3)$_3$], 27.34 (CH_3), 23.14 (CH_3), 16.66 (d, $^3J_{C,P}$ = 3.39 Hz, CH_2CH_3), 16.28 (d, $^3J_{C,P}$ = 6.04 Hz, CH_2CH_3) ppm. ^{31}P NMR: δ = 25.55 ppm. $C_{18}H_{38}NO_6P$ (395.47): C 54.67, H 9.69, N 3.54; found C 54.80, H 9.75, N 3.54.

2-Methyl-2-[*N*-*tert*-butyl-*N*-(1-diethoxyphosphoryl-2,2-dimethylpropyl)aminoxy]propionitrile (24g): Compound **24g** (1.45 g, 4.04 mmol, 60%) was obtained as a pale yellow solid after allowing 2-bromo-2-methylpropionitrile (1.51 g, 10.2 mmol), SG1 (2 g, 6.8 mmol) in benzene (20 mL) and CuBr (1.47 g, 10.2 mmol), Cu^0 (0.65 g, 10.2 mmol) and PMDETA (3.52 g, 20.4 mmol) in benzene (20 mL) to react for 0.5 h at room temp. Eluent: pentane/ethyl acetate, 3:1. ^{1}H NMR: δ = 4.27–3.88 (m, 4 H, CH_2), 3.37 (d, $^2J_{H,P}$ = 27 Hz, 1 H, CHP), 1.89 (s, 3 H, Me), 1.71 (s, 3 H, Me), 1.31 (t, $^3J_{H,H}$ = 6 Hz, 3 H, CH_3), 1.30 (t, $^3J_{H,H}$ = 6 Hz, 3 H, CH_3), 1.25 (s, 9 H, *t*Bu), 1.24 (s, 9 H, *t*Bu) ppm. ^{13}C NMR: δ = 120.8 (C≡N), 77.2 (OC), 69.0 (d, $^1J_{C,P}$ = 138.1 Hz, CHP), 62.3 (CN), 60.95 (d, $^2J_{C,P}$ = 6.8 Hz, CH_2), 58.57 (d, $^2J_{C,P}$ = 7.6 Hz, CH_2), 35.45 (d, $^2J_{C,P}$ = 5.3 Hz, PC*C*), 29.8 [d, $^3J_{C,P}$ = 7.55 Hz, PCC(CH_3)$_3$], 28.5 [NC(CH_3)$_3$], 28.3 (CH_3), 27.8 (CH_3), 16.03 (d, $^3J_{C,P}$ = 5.3 Hz, CH_2CH_3), 15.62 (d, $^3J_{C,P}$ = 6.0 Hz, CH_2CH_3) ppm. ^{31}P NMR: δ = 24.09 ppm. $C_{17}H_{35}N_2O_4P$ (362.44): C 56.33, H 9.73, N 7.73; found C 55.94, H 9.61, N 7.95.

Phenyl 2-Methyl-2-[*N*-*tert*-butyl-*N*-(1-diethoxyphosphoryl-2,2-dimethylpropyl)aminoxy]propionate (24dPh): Compound **24dPh** (1.09 g, 2.38 mmol, 35%) was obtained as a white solid after allowing 2-bromo-2-methylpropionic acid phenyl ester (2.48 g, 10.2 mmol), SG1 (2 g, 6.8 mmol) in benzene (20 mL) and CuBr (1.47 g, 10.2 mmol), Cu^0 (0.65 g, 10.2 mmol) and PMDETA (3.52 g, 20.4 mmol) in benzene (20 mL) to react for 0.5 h at room temp. After drying under high vacuum (6×10^{-2} mbar) the residue was precipitated in pentane at –18 °C. ^{1}H NMR: δ = 7.48–7.28 (m, 2 H, CH_{aryl}), 7.30–7.22 (m, 1 H, CH_{aryl}), 7.13–7.00 (m, 2 H, CH_{aryl}), 4.48–4.25 (m, 2 H, CH_2), 4.14–3.87 (m, 2 H, CH_2), 3.32 (d, $^2J_{H,P}$ = 24 Hz, 1 H, CHP), 1.85 (s, 3 H, CH_3), 1.78 (s, 3 H, CH_3), 1.46 (t, $^3J_{H,H}$ = 6 Hz, 3 H), 1.30 (t, $^3J_{H,H}$ = 6 Hz, 3 H), 1.23 (s, 9 H, *t*Bu), 1.19 (s, 9 H, *t*Bu) ppm. ^{13}C NMR: δ = 175.31 (C=O), 150.76 (C_{aryl}-O), 129.38 (CH_{aryl}), 125.72 (CH_{aryl}), 121.16 (CH_{aryl}), 83.76 (OC), 70.03 (d, $^1J_{C,P}$ = 138.1 Hz, CHP), 62.26 (CN), 61.79 (d, $^2J_{C,P}$ = 6.03 Hz, CH_2), 58.58 (d, $^2J_{C,P}$ = 8.30 Hz, CH_2), 35.94 (d, $^2J_{C,P}$ = 6.8 Hz, PC*C*), 29.99 [d, $^3J_{C,P}$ = 6.03 Hz, PCC(CH_3)$_3$], 28.41 [NC(CH_3)$_3$], 28.18 (CH_3), 22.22 (CH_3), 16.58 (d, $^3J_{C,P}$ = 6.04 Hz, CH_2CH_3), 16.16 (d, $^2J_{C,P}$ = 6.79 Hz, CH_2CH_3) ppm. ^{31}P NMR: δ = 25.38 ppm. $C_{23}H_{40}NO_6P$ (457.54): C 60.38, H 8.81, N 3.06; found C 60.56, H 8.45, N 3.10.

2-[*N*-*tert*-Butyl-*N*-(1-diethoxyphosphoryl-2,2-dimethylpropyl)aminoxy]acetic Acid (24u): Alkoxyamine **24u** was obtained as white solid (50% yield). ^{1}H NMR: δ = 4.70 (d, $^2J_{H,H}$ = 18 Hz, CH_2), 4.63 (d, $^2J_{H,H}$ = 15 Hz, CH_2), 4.32–3.97 (m, 4 H, CH_2), 3.25 (d, $^2J_{H,H}$ = 24 Hz, 1 H, CHP), 1.34 (dt, $^3J_{H,H}$ = 6 Hz, $^4J_{H,P}$ = 3 Hz, 6 H, CH_3), 1.17 (s, 9 H, *t*Bu), 1.14 (s, 9 H, *t*Bu) ppm. ^{13}C NMR: δ = 170.53 (C=O), 77.01 (OC), 68.60 (d, $^1J_{C,P}$ = 138.9 Hz, CH), 62.88 (s, CN), 62.41 (d, $^2J_{C,P}$ = 7.55 Hz, CH_2), 60.62 (d, $^2J_{C,P}$ = 8.30 Hz, CH_2), 35.76 (d, $^2J_{C,P}$ = 5.28 Hz, PC*C*), 29.59 [d, $^3J_{C,P}$ = 6.04 Hz, PCC(CH_3)$_3$], 28.06 [s, NC(CH_3)$_3$], 16.34 ($^3J_{C,P}$ = 5.28 Hz, CH_2CH_3)$_3$, 16.11 ($^3J_{C,P}$ = 6.79 Hz, CH_2CH_3)$_3$ ppm. ^{31}P NMR: δ = 28.54 ppm.

2,2-Dimethyl-4-[*N*-*tert*-butyl-*N*-(1-diethoxyphosphoryl-2,2-dimethylpropyl)aminoxy]-4-*n*-butoxycarbonylpentanoic Acid (24v): Alkoxyamine **24s** (2 g, 5.25 mmol) and *n*-butyl acrylate (0.67 g, 5.25 mmol) were dissolved in *tert*-butyl alcohol (*t*BuOH) (1 M solution). Then the solution was deoxygenated by nitrogen bubbling and heated for 6 h at 80 °C whilst stirring. The reaction mixture was then concentrated under reduced pressure and the residue was taken up in pentane to afford after filtration **24v** (1.74 g, 3.42 mmol, 65%) as a white solid. One diastereoisomer was obtained as a white crystal. ^{1}H NMR: δ = 10.00 (br., 1 H, OH), 4.54–4.49 (m, 1 H, CHO), 4.27–3.90 (m, 6 H, 3 CH_2), 3.29 (d, $^2J_{H,P}$ = 24 Hz, 1 H, CHP), 2.58–2.52 (m, 1 H, CH_2), 2.24–2.16 (m, 1 H, CH_2), 1.64–1.57 (m, 2 H, CH_2), 1.43–1.46 (m, 2 H, CH_2), 1.32–1.23 (m, 6 H, 2 OCH_2CH_3), 1.22 (s, 6 H, 2 CH_3), 1.16 [s, 9 H, $C(CH_3)_3$], 1.08 [s, 9 H, $C(CH_3)_3$], 0.93 (t, $^3J_{H,H}$ = 9 Hz, 3 H, CH_3) ppm. ^{13}C NMR: δ = 181.53 (COOH), 172.70 (C=O), 83.48 (CHO), 69.50 (d, $^1J_{C,P}$ = 139.6 Hz, CHP), 64.19 (OCH_2), 62.00 (d, $^2J_{C,P}$ = 6.04 Hz, OCH_2CH_3), 61.49 (CN), 58.88 (d, $^2J_{C,P}$ = 7.55 Hz, OCH_2CH_3), 40.91 (CCH_2), 40.04 [$C(CH_3)_2$], 35.47 (d, $^2J_{C,P}$ = 5.28 Hz, PC*C*), 30.11 (CH_2), 29.61 [d, $^3J_{C,P}$ = 5.28 Hz, $PCC(CH_3)_3$], 27.79 (CH_3), 22.94 (CH_3), 19.00 (CH_2), 16.24 (d, $^2J_{C,P}$ = 6.79 Hz, CH_2CH_3), 16.02 (d, $^2J_{C,P}$ = 6.79 Hz, CH_2CH_3), 13.51 (CH_3) ppm. ^{31}P NMR: δ = 24.48 ppm. MS (ESI): 509.9 $[M + H]^+$, calcd. 509.3; 526.9 $[M + NH_4]^+$, calcd. 527.3; 532.2 $[M + Na]^+$, calcd. 532.3; 548.1 $[M + K]^+$, calcd. 548.3.

Computational Method: All calculations were performed with the Gaussian 03 molecular orbital package.[62] Geometry optimizations were carried out without constraints at the B3LYP/6-31G(d) level of theory. Vibrational frequencies were calculated at the B3LYP/6-31G(d) level to determine the nature of the located stationary points. Frequency calculations were performed to confirm that the geometry was a minimum (0 imaginary frequency). The single-point energies were then calculated at the B3P86/6-311++G(d,p) level of theory.

The optimized preferred conformations of the model compounds were analysed by the natural bond orbitals method[63] included in the Gaussian 03 package (NBO, 3.1) in order to determine the incidence of stereoelectronic effects.

Acknowledgments

Atofina, the University of Provence and the CNRS are thanked for their financial support. S. R. A. M. thanks Dr. G. Ananchenko for fruitful discussions.

[1] D. H. Solomon, E. Rizzardo, P. Cacioli, *US Patent* 4,581,429, **1986**, *Eur. Pat. Appl.* 135280, **1985** [*Chem. Abstr.* **1985**, *102*, 221335q].
[2] M. K. Georges, R. P. N. Veregin, P. M. Kazmaier, G. K. Hamer, *Macromolecules* **1993**, *26*, 2987–2988.
[3] C. J. Hawker, *Acc. Chem. Res.* **1997**, *30*, 373–382.
[4] C. J. Hawker, A. W. Bosman, E. Harth, *Chem. Rev.* **2001**, *101*, 3661–3688 and references cited therein.
[5] D. Greszta, K. Matyjaszewski, *Macromolecules* **1996**, *29*, 7661–7670 and references cited therein.
[6] H. Fischer, M. Souaille, *Chimia* **2001**, *55*, 109–113.
[7] T. Fukuda, A. Goto, K. Ohno, *Macromol. Rapid Commun.* **2000**, *21*, 151–165.
[8] H. Fischer, *Chem. Rev.* **2001**, *101*, 3581–3610 and references cited therein.
[9] A. Goto, T. Fukuda, *Prog. Polym. Sci.* **2004**, *29*, 329–385 and references cited therein.
[10] T. Fukuda, A. Goto, Y Tsujii in *Handbook of Radical Polymerization* (Eds.: K. Matyjaszewski, T. P. Davis), Wiley, New York, **2002**, pp. 407–462 and references cited therein.
[11] H. Fischer, *ACS Symp. Ser.* **2003**, *854*, 10–23.
[12] K. Matyjaszewski, *Controlled Radical Polymerization*, American Chemical Society: Washington, DC, **1998**, vol. 685.
[13] K. Matyjaszewski (Ed.), *Controlled-Living Radical Polymerization: Progress in ATRP, NMP, and RAFT*, American Chemical Society: Washington, DC, **2000**, vol. 768.
[14] K. Matyjaszewski, *Macromol. Symp.* **2001**, *174*, 51.
[15] G. Moad, E. Rizzardo, *Macromolecules* **1995**, *28*, 8722–8728.
[16] S. Grimaldi, F. Le Moigne, J.-P. Finet, P. Tordo, P. Nicol, M. Plechot, *International Patent*, WO 96/24620, **1996**..
[17] D. Benoit, V. Chaplinski, R. Braslau, C. J. Hawker, *J. Am. Chem. Soc.* **1999**, *121*, 3904–3920.
[18] M.-O. Zink, A. Kramer, P. Nesvadba, *Macromolecules* **2000**, *33*, 8106–8108.
[19] A. Kramer, P. Nesvadba, DE 19909767, **1999** [*Chem. Abstr.* **1999**, *131*, 229170].
[20] J.-L. Couturier, O. Guerret, D. Gigmes, S. Marque, F. Chauvin, P.-E. Dufils, D. Bertin, P. Tordo, FR 2843394, **2004**; WO 2004014926, **2004**.
[21] C. Wetter, J. Gierlich, C. A. Knoop, C. Müller, T. Schulte, A. Studer, *Chem. Eur. J.* **2004**, *10*, 1156–1166.
[22] E. Drockenmuller, J.-M. Catala, *Macromolecules* **2002**, *35*, 2461–2466.
[23] D. Bertin, P.-E. Dufils, D. Gigmes, Y. Guillaneuf, S. R. A. Marque, P. Tordo, unpublished results.
[24] S. Marque, C. Le Mercier, P. Tordo, H. Fischer, *Macromolecules* **2000**, *33*, 4403–4410.
[25] P. Marsal, M. Roche, P. Tordo, P. de Sainte Claire, *J. Phys. Chem. A* **1999**, *103*, 29899–29905.
[26] M. V. Ciriano, H.-G. Korth, W. B. van Scheppingen, P. Mulder, *J. Am. Chem. Soc.* **1999**, *121*, 6375–6381.
[27] S. Marque, H. Fischer, E. Baier, A. Studer, *J. Org. Chem.* **2001**, *66*, 1146–1156.
[28] C. Le Mercier, J.-F. Lutz, S. Marque, F. Le Moigne, P. Tordo, P. Lacroix-Desmazes, B. Boutevin, J. L. Couturier, O. Guerret, R. Martschke, J. Sobek, H. Fischer, *ACS Symp. Ser.* **2000**, *768*, 108–122.
[29] S. Marque, *J. Org. Chem.* **2003**, *68*, 7582–7590.
[30] A. Goto, T. Fukuda, *Macromol. Chem. Phys.* **2000**, *201*, 2138–2142.
[31] W. G. Skene, S. T. Belt, T. J. Connolly, P. Hahn, J. C. Scaiano, *Macromolecules* **1998**, *31*, 9103–9105.
[32] S. Acerbis, E. Beaudouin, D. Bertin, D. Gigmes, S. Marque, P. Tordo, *Macromol. Chem. Phys.* **2004**, *205*, 973–978.
[33] D. Bertin, D. Gigmes, S. R. A. Marque, P. Tordo, *Macromolecules* **2005**, *38*, 2638–2650.
[34] D. Bertin, D. Gigmes, C. Le Mercier, S. R. A. Marque, P. Tordo, *J. Org. Chem.* **2004**, *69*, 4925–4930.
[35] D. Bertin, D. Gigmes, J. Peri, S. R. A. Marque, S. Milardo, P. Tordo, *Collect. Czech. Chem. Commun.* **2004**, *69*, 2223–2238.
[36] D. Bertin, D. Gigmes, S. R. A. Marque, R. Maurin, P. Tordo, *J. Polym. Sci., Part A: Polym. Chem.* **2004**, *42*, 3504–3515.
[37] G. S. Ananchenko, S. Marque, D. Gigmes, D. Bertin, P. Tordo, *Org. Biomol. Chem.* **2004**, *2*, 709–7014.
[38] K. Matyjaszewski, B. E. Woodworth, X. Zhang, S. Gaynor, Z. Metzner, *Macromolecules* **1998**, *31*, 5955–5957.
[39] D. Bertin, P.-E. Dufils, D. Gigmes, S. A. R. Marque, P. Tordo, unpublished results.
[40] D. Bertin, D. Gigmes, S. Marque, P. Tordo, *e-Polymers* **2003**, paper no. 2.
[41] O. Exner, M. Charton, V. Galkin, *J. Phys. Org. Chem.* **1999**, *12*, 289.
[42] M. Charton, *Prog. Phys. Org. Chem.* **1981**, *13*, 119–251.
[43] M. Charton, *Top. Curr. Chem.* **1983**, *114*, 57–91.
[44] J. J. Brocks, H.-D. Beckhaus, A. L. J. Beckwith, C. Rüchardt, *J. Org. Chem.* **1998**, *63*, 1935–1943.

[45] Y.-R. Luo, *Handbook of Bond Dissociation Energies in Organic Compounds*, CRC Press, Boca Raton, FL, **2003**.
[46] M. Charton, *Adv. Quant. Struct.-Prop. Rel.* **1996**, *1*, 171–219.
[47] M. Charton, *Stud. Org. Chem.* **1991**, *42*, 629–692.
[48] G. Ananchenko, D. Bertin, D. Gigmes, P. Lagarde, S. R. A. Marque, E. Revalor, P. Tordo, *J. Phys. Org. Chem.*, submitted.
[49] CCDC-235453 (for **24s**), -235454 (for **24dPh**), -275836 [for (*RR*/*SS*)-**17**], -275837 [for (*RS*/*SR*)-**17**], and -277677 [for (*RS*/*SR*)-**24eMe**] contain the supplementary crystallographic data for this paper. These data can be obtained free of charge from The Cambridge Crystallographic Data Centre via www.ccdc.cam.ac.uk/data_request/cif.
[50] M. Raban, D. Kost, *Tetrahedron* **1984**, *40*, 3345–3381.
[51] TIPNO: 2,2,5,5-tetramethyl-4-phenyl-3-azahexane-3-oxyl radical; DBNO: di-*tert*-butyl nitroxyl radical.
[52] The value of k_d for **24fMe** was estimated at 150 °C by ESR spectroscopy using the initial slope approximation[34] and it has been reported that SG1 is not stable for long above 120 °C.[24]
[53] D. Bertin, P.-E. Dufils, D. Gigmes, B. Giovanetti, Y. Guillaneuf, S. A. R. Marque, P. Tordo, unpublished results.
[54] S. Grimaldi, D. Siri, J.-P. Finet, P. Tordo, *Acta Crystallogr., Sect. C: Crystal Struct. Commun.* **1998**, *54*, 1712.
[55] S. Acerbis, D. Bertin, B. Boutevin, D. Gigmes, P. Lacroix-Desmazes, C. Le Mercier, J.-F. Lutz, S. R. A. Marque, D. Siri, P. Tordo, *Helv. Chim. Acta*, paper submitted for publication.
[56] ^{31}P NMR analysis in liquid and in the solid phase showed reversible growth of peaks when the sample was heated.
[57] A. Studer, K. Harms, C. Knoop, C. Müller, T. Schulte, *Macromolecules* **2004**, *37*, 27. Recently, these authors published data that did not correlate with the relationship developed in ref.[29]
[58] Alkoxyamines recently prepared by our group did not correlate with the relationship developed in ref.[29].
[59] W. L. F. Armarego, C. L. L. Chai, *Purification of Laboratory Chemicals*, 5th ed., Butterworth Heinemann, Amsterdam, **2003**.
[60] H. Schick, R. Ludwig, K. Kleiner, A. Kunath, *Tetrahedron* **1995**, *51*, 2939–2946.
[61] P. Couvreur, A. Bruylants, *J. Org. Chem.* **1953**, *18*, 501–506.
[62] M. J. Frisch, G. W. Trucks, H. B. Schlegel, G. E. Scuseria, M. A. Robb, J. R. Cheeseman, J. A. Montgomery Jr., T. Vreven, K. N. Kudin, J. C. Burant, J. M. Millam, S. S. Iyengar, J. Tomasi, V. Barone, B. Mennucci, M. Cossi, G. Scalmani, N. Rega, G. A. Petersson, H. Nakatsuji, M. Hada, M. Ehara, K. Toyota, R. Fukuda, J. Hasegawa, M. Ishida, T. Nakajima, Y. Honda, O. Kitao, H. Nakai, M. Klene, X. Li, J. E. Knox, H. P. Hratchian, J. B. Cross, C. Adamo, J. Jaramillo, R. Gomperts, R. E. Stratmann, O. Yazyev, A. J. Austin, R. Cammi, C. Pomelli, J. W. Ochterski, P. Y. Ayala, K. Morokuma, G. A. Voth, P. Salvador, J. J. Dannenberg, V. G. Zakrzewski, S. Dapprich, A. D. Daniels, M. C. Strain, O. Farkas, D. K. Malick, A. D. Rabuck, K. Raghavachari, J. B. Foresman, J. V. Ortiz, Q. Cui, A. G. Baboul, S. Clifford, J. Cioslowski, B. B. Stefanov, G. Liu, A. Liashenko, P. Piskorz, I. Komaromi, R. L. Martin, D. J. Fox, T. Keith, M. A. Al-Laham, C. Y. Peng, A. Nanayakkara, M. Challacombe, P. M. W. Gill, B. Johnson, W. Chen, M. W. Wong, C. Gonzalez, J. A. Pople, *Gaussian 03, Revision C.02*, Gaussian, Inc., Wallingford, CT, **2004**.
[63] A. E. Reed, L. A. Curtiss, F. Weinhold, *Chem. Rev.* **1988**, *88*, 899.

Received: September 26, 2005
Published Online: January 27, 2006

